The Scientific Temper (2024) Vol. 15 (spl): 132-140

E-ISSN: 2231-6396, ISSN: 0976-8653

Doi: 10.58414/SCIENTIFICTEMPER.2024.15.spl.16

https://scientifictemper.com/

RESEARCH ARTICLE

Improving image quality assessment with enhanced denoising autoencoders and optimization methods

V. Karthikeyan*, C. Jayanthi

Abstract

In the field of image quality assessment, effective noise reduction is critical for enhancing the perceptual quality of images and improving the accuracy of subsequent analyses. This study proposes an enhancement to denoising autoencoders (DAEs) through optimization techniques aimed at significantly improving image quality assessment outcomes. Traditional DAEs, while effective in reconstructing clean images from noisy inputs, can sometimes fail to adequately preserve intricate image details and structures, which are essential for quality evaluation. Our approach incorporates optimization strategies, including adaptive learning rates, regularization techniques, and advanced loss functions, to refine the DAE architecture and improve its denoising capabilities. By training the enhanced model on diverse datasets containing various noise types and image content, we achieve superior performance in noise reduction. The effectiveness of the optimized denoising autoencoder is rigorously evaluated using standard image quality metrics, including Peak signal-to-noise ratio (PSNR), structural similarity index (SSIM), and other perceptual quality measures. Results demonstrate a marked improvement in image quality, leading to more reliable assessments in various applications, including medical imaging, remote sensing, and multimedia content. This work highlights the potential of leveraging optimization techniques to enhance denoising autoencoders, thereby providing a robust solution for improving image quality assessment methodologies.

Keywords: Image quality assessment, Denoising autoencoders, Autoencoders, Image processing, Deep learning.

Introduction

Image quality assessment (IQA) plays a crucial role in the field of computer vision, serving as a key enabler for a variety of applications such as image enhancement, medical diagnostics, surveillance, and multimedia processing. As digital imaging continues to advance, the need for precise, efficient, and automated IQA systems becomes increasingly vital. Traditional methods of IQA, often based on pixel-based metrics like Peak Signal-to-Noise Ratio (PSNR) and Structural Similarity Index (SSIM), are limited in their capacity to capture nuanced distortions and high-level features that contribute to perceived image quality. Consequently, these conventional approaches may fall short of accurately assessing the quality of images processed in dynamic, high-noise environments. To address these limitations, recent research has pivoted towards leveraging machine learning (ML) models, especially neural networks, to develop more robust IQA frameworks. Among these, autoencoders, a specialized type of neural network designed for dimensionality reduction and unsupervised learning, have shown promise in addressing complex quality assessment challenges, Ma, K., & Fang, Y. (2021, October), Guo, H., Bin, Y., Hou, Y., Zhang, Q., & Luo, H. (2021).

Denoising autoencoders (DAEs), in particular, offer a unique advantage by reconstructing high-quality images from noisy or degraded versions, effectively removing unwanted artifacts and distortions. However, conventional DAEs face inherent limitations in balancing quality restoration and processing efficiency, leading to challenges in real-world IQA applications. This research aims to enhance the capabilities of DAEs by integrating advanced optimization methods, resulting in an improved framework for image quality assessment that is more precise and reliable. Optimization techniques can significantly

PG and Research Department of Computer Science, Government Arts College (Autonomous), Karur-5. (Affiliated to Bharathidasan University, Tiruchirappalli), Tamilnadu, India

***Corresponding Author:** V. Karthikeyan, PG and Research Department of Computer Science, Government Arts College (Autonomous), Karur-5. (Affiliated to Bharathidasan University, Tiruchirappalli), Tamilnadu, India, E-Mail: sriramkarthikeyan92@gmail.com

How to cite this article: Karthikeyan, V., Jayanthi, C. (2024). Improving image quality assessment with enhanced denoising autoencoders and optimization methods. The Scientific Temper, **15**(spl):132-140.

Doi: 10.58414/SCIENTIFICTEMPER.2024.15.spl.16

Source of support: Nil

Conflict of interest: None.

Received: 04/09/2024 **Accepted:** 18/09/2024 **Published:** 16/10/2024

elevate the performance of DAEs by fine-tuning their hyperparameters and guiding the learning process toward an optimal denoising outcome. Combining DAEs with robust optimization algorithms such as Particle Swarm Optimization (PSO) [3], Genetic Algorithms (GA), or Cuckoo search (CS) can further improve the model's ability to capture subtle details and structural information within images, which are essential for high-fidelity image quality assessment, Hossain, M. M., Hasan, M. M., Rahim, M. A., Rahman, M. M., Yousuf, M. A., Al-Ashhab, S., ... & Moni, M. A. (2022), Merzougui, N., & Djerou, L. (2021), WangNo, N., Chiewchanwattana, S., & Sunat, K. (2023).

This research proposes an enhanced denoising autoencoder (EDAE) model equipped with optimization techniques to achieve superior IQA results. The EDAE architecture incorporates advanced optimization algorithms to dynamically adjust the model parameters, optimizing the balance between denoising efficiency and quality retention. By adopting a dual approach that combines deep learning with optimization, the proposed EDAE framework is designed to address the limitations of traditional DAEs, offering a more accurate and adaptive solution to image quality assessment. Specifically, this study will evaluate the impact of optimization-enhanced DAEs on IQA performance using a variety of image datasets with varying levels of noise and quality degradation.

This study contributes to the field of IQA by presenting a novel framework that leverages the strengths of both DAEs and optimization methods, paving the way for future research in adaptive, intelligent IQA systems. The proposed EDAE framework not only enhances image denoising capabilities but also brings adaptability to changing noise patterns and varying image quality demands in practical applications. This research further investigates the potential of using optimization techniques to streamline computational efficiency in deep learning models, presenting a dual benefit of quality improvement and performance enhancement. Ultimately, the findings of this study aim to establish a foundation for developing scalable, real-time IQA systems capable of operating in diverse and challenging environments, thereby extending the utility of IQA in fields as diverse as medical imaging, autonomous driving, and multimedia technology.

Denoising Autoencoders

Denoising autoencoders (DAEs) are a specialized type of neural network designed to learn efficient representations of data by reconstructing clean inputs from corrupted or noisy versions. As a variant of traditional autoencoders, DAEs have gained considerable attention in various fields, including image processing, natural language processing, and anomaly detection. Understanding the mechanisms, architectures, and applications of denoising autoencoders is crucial for leveraging their potential in improving image quality assessment and other related tasks, Cui, H., & Zdeborová, L. (2023), Gheller, C., & Vazza, F. (2022).

Autoencoders are unsupervised neural networks composed of two main components: an encoder and a decoder. The encoder compresses the input data into a lower-dimensional representation (latent space), while the decoder reconstructs the input data from this representation. The primary objective is to minimize the reconstruction error between the input and the output. Traditional autoencoders are effective for tasks like dimensionality reduction and feature learning but may not handle noisy data well, Lee, W. H., Ozger, M., Challita, U., & Sung, K. W. (2021).

In real-world scenarios, data often contains noise, which can significantly degrade the performance of machine learning models. For instance, in image processing, noise can arise from various sources, such as sensor imperfections, transmission errors, or environmental factors. Denoising autoencoders address this issue by training the model to reconstruct clean images from corrupted inputs. This process involves adding noise to the input data during training and teaching the model to recover the original, noise-free data.

A typical DAE architecture consists of the following components:

Corruption Process

The input data is intentionally corrupted by adding noise (e.g., Gaussian noise, salt-and-pepper noise, or random pixel masking) to create a degraded version.

Encoder

The corrupted input is fed into the encoder, which compresses the data into a lower-dimensional representation. This representation captures the essential features of the input while discarding noise.

Decoder

The decoder reconstructs the original clean data from the latent representation. The model is trained to minimize the difference between the reconstructed output and the original clean input, using loss functions such as mean squared error (MSE) or binary cross-entropy.

Training a DAE involves optimizing the network parameters using backpropagation and stochastic gradient descent (SGD) or its variants. The key is to ensure that the model learns to ignore the noise and focus on the underlying patterns in the data. Hyperparameter tuning, including learning rate, batch size, and architecture design (number of layers, activation functions), is essential for achieving optimal performance, Tian, Y., Zhang, Y., & Zhang, H. (2023), Kumar, V. S., & Jayalakshmi, V. (2021, September).

Step by Step Procedure for Denoising AutoEncoders (DAE)

Denoising autoencoders (DAEs) are a powerful tool for image quality assessment (IQA) as they can effectively learn to remove noise from images, improving their perceptual quality.

Step 1: Overview of Denoising Autoencoders

DAEs are designed to reconstruct clean images from noisy or corrupted versions. The fundamental components of a DAE include:

- *Input Layer*

Receives the corrupted image.

- *Encoder*

Transforms the input into a lower-dimensional latent representation.

- *Decoder*

Reconstructs the clean image from the latent representation.

The training process involves adding noise to the original images and teaching the model to recover the original images as accurately as possible.

Step 2: Corruption Process

To train a DAE, a corruption process is applied to the input images. The common types of noise include:

- *Gaussian Noise*

This is a common type of noise, represented as: where x is the original image, $\tilde{x}$ is the corrupted image, and $N(0,\sigma^2)$ represents Gaussian noise with mean 0 and variance σ^2.

$$\tilde{x} = x + N(0,\sigma^2) \quad (1)$$

- *Salt-and-Pepper Noise*

Randomly replaces some pixels in the image with black or white pixels.

Step 3: Encoder and Decoder Architecture

The architecture of the encoder and decoder can vary, but a common approach is to use fully connected layers or convolutional layers for images. The encoder maps the input $\tilde{x}$ to a latent representation z: where f is the encoding function, W_e represents the weights, and b_e denotes the bias.

$$z = f(\tilde{x}; W_e, b_e) \quad (2)$$

The decoders reconstruct the image from the latest representation, where g is the decoding function; W_d and b_d are the corresponding weights and biases.

$$\hat{x} = g(\tilde{x}; W_d, b_d) \quad (3)$$

Step 4: Loss Function

The objective of training a DAE is to minimize the reconstruction error between the original image x and the reconstructed image $\hat{x}$. The loss function commonly used is the mean square error (MSE): where N is the number of images in the training set, and ||·|| denotes the L2 norm.

$$L = \frac{1}{N}\sum_{i=1}^{N}\|x_i - \hat{x}_i\|^2 \quad (4)$$

Step 5: Optimization

To minimize the loss function, optimization algorithms such as stochastic gradient descent (SGD) or Adam are used. The update rules for weights and biases can be expressed as: where η is the learning rate.

$$W_e \leftarrow W_e - \eta\frac{\partial L}{\partial W_e} \quad (5)$$

$$b_e \leftarrow b_e - \eta\frac{\partial L}{\partial b_e} \quad (6)$$

$$W_d \leftarrow W_d - \eta\frac{\partial L}{\partial W_d} \quad (7)$$

$$b_d \leftarrow b_d - \eta\frac{\partial L}{\partial b_d} \quad (8)$$

Cuckoo Search Optimization (CSO)

Cuckoo search optimization (CSO) is a relatively recent metaheuristic optimization algorithm inspired by the brood parasitism behavior of certain cuckoo species. This algorithm was proposed by Xin-She Yang and Suash Deb in 2009. CSO is particularly effective for solving complex optimization problems in various domains, including engineering, data mining, and machine learning. The Cuckoo Search algorithm is based on the following three main ideas: Sharma A., Sharma, A., Chowdary, V., Srivastava, A., & Joshi, P. (2021), Mohiz, M. J., Baloch, N. K., Hussain, F., Saleem, S., Zikria, Y. B., & Yu, H. (2021), Al-Abaji, M. A. (2021):

Brood Parasitism

Some cuckoo species lay their eggs in the nests of other birds, leaving the host to raise their chicks. If a host discovers a foreign egg, it can either reject it or abandon the nest altogether.

Levy Flight

The algorithm employs a random walk pattern known as Levy flight for exploration, which allows for a more effective search of the solution space. Levy flights are random walks where the step lengths are drawn from a specific distribution, enabling long jumps in the search space while maintaining local search capabilities.

Exploration and Exploitation

CSO balances exploration (searching new areas of the solution space) and exploitation (refining known good solutions) to effectively navigate complex optimization landscapes.

Algorithm Steps

The basic steps of the Cuckoo search algorithm are as follows:

Step 1: Initialization

- Define the objective function to be optimized.
- Initialize a population of «cuckoos» (solutions) randomly within the search space.
- Set parameters such as the number of iterations, population size, and discovery rate.

Step 2: Generate New Solutions

- For each cuckoo, a new solution is generated using the Levy flight mechanism, where x_i is the current

solution (cuckoo), α is a step size, $Levy(\lambda)$ is a random step length drawn from the Levy distribution with parameter λ.

$$x_i^{new} = x_i + \alpha . Levy(\lambda) \quad (9)$$

Step 3: Evaluate and Replace

- Evaluate the fitness of the new solution.
- If the new solution is better than the worst solution in the population, replace the worst solution with the new one.
- If a host bird detects an egg from a foreign cuckoo (based on a predefined discovery rate p), it may replace it with a random solution.

Step 4: Termination

- Repeat steps 2 and 3 for a predefined number of iterations or until convergence criteria are met.

Step 5: Return the Best Solution

- After all iterations, the algorithm returns the best solution found.

Proposed Optimization-Based Denoising Autoencoders (Odae) Approach

The integration of denoising autoencoders (DAEs) with CSO creates a synergistic framework for enhancing image quality assessment and noise reduction capabilities. This innovative approach leverages the strengths of both techniques—DAEs for their effective feature extraction and noise removal and CSO for its robust optimization abilities.

Step 1: Data Preparation

- *Dataset Preparation*

Gather a dataset of clean images $X = (x_1, x_2, \ldots, x_n)$

- *Adding Noise*

Introduce noise to the images to create a corrupted version $\tilde{X} = \{\tilde{x}_1, \tilde{x}_2, \ldots, \tilde{x}_n\}$ where $\tilde{x}_i = x_i + N(0, \sigma^2)$ for Gaussian noise.

Step 2: Initialize the Denoising Autoencoder (DAE) Architecture

Define Layers:

- *Encoder*

Maps noisy input $\tilde{x}$ to a latent representation z with the equation (2).

- *Decoder*

Reconstructs the original image x from z with the equation (3)

- *Activation Functions*

Typically, ReLU or sigmoid functions are used in the encoder and decoder layers.

Step 3: Define the Objective Function for the DAE

The DAE's primary objective is to minimize the reconstruction loss, defined by the MSE between the original images x and the reconstructed images $\hat{x}$ with the equation (4).

Step 4: Initialize the Cuckoo Search Optimization (CSO)

- *Define Parameters for CSO*
- Population Size: Number of cuckoos (solutions).
- Discovery Rate (p_a): The probability that a host will discover a foreign egg and replace it.
- Levy Flight Parameters: Parameters governing the Levy flight for exploration.

- *Initialize Population*
- Each cuckoo represents a set of weights and biases (W_e, b_e, W_d, b_d) for the DAE.
- Randomly initialize each cuckoo with values within a defined range.

Step 5: Iterative Optimization with Cuckoo Search

- *Generate New Solutions Using Levy Flight*

For each cuckoo (solution), generate a new solution via Levy flight with the equation (9).

- *Evaluate the Fitness of Each Solution*
- Compute the reconstruction loss for each cuckoo's parameters using the DAE's objective using equation (4).
- This loss serves as the fitness function for each cuckoo. Lower fitness values indicate better solutions.

- *Replace Worst Solutions*
- Identify the worst-performing solutions (highest loss) and replace them with new solutions generated randomly.
- With a probability p_a, randomly replace some solutions to avoid local minima, analogous to a host bird discovering foreign eggs.

- *Select the Best Solution*

Retain the best-performing solution (i.e., the set of weights and biases with the lowest reconstruction loss) at the end of each iteration.

- *Termination*

Repeat steps 1 to 4 for a fixed number of iterations or until convergence criteria are met (e.g., a sufficiently low reconstruction loss).

Step 6: Final Training and Fine-Tuning of the Optimized DAE

- *Optimized Training*
- Use the best parameters obtained from CSO as the starting point for further training on the complete dataset.
- Fine-tune the network to minimize the reconstruction loss further, ensuring the model is robust for various noise levels.

Result And Discussion

The following are the benchmark images are considered to validate the proposed ODAE algorithm in the pre-processing

step (Figure 1). To evaluate the proposed algorithm, the performance of the ODAE algorithm is compared with the following denoising algorithms like non-local means (NLM), K means-singular vector decomposition (K-SVD), block matching and 3D filtering (BM3D), Zhang, X. (2022), Žalik, K. R., & Žalik, M. (2023, July), Do, Y., Cho, Y., Kang, S. H., & Lee, Y. (2022).

Parameter Setting

The parameters set for the proposed ODAE algorithm is followed as: the noise variance δ in the range of [5, 15, 25, 40, 60, 80]. The performance metrics like peak signal to noise ratio (PSNR), structural similarity (SSIM), and figure of merit (FOM) are used to validate the proposed ODAE method.

The four noisy images such as Monarch, Baboon, Airplane and Lena, are considered for evaluating the proposed ODAE method. The following Figure 2 represents the noisy images of Lena, Airplane, Monarch, and Baboon.

From Table 1, the proposed ODAE method gives their maximum values of PNSR, FOM and SSIM with the noise level of δ = 60. The PNSR value for proposed method is 27.50 dB, FOM is 0.4598 and SSIM is 0.8876.

The following Table 2 depicts the performance comparison of the proposed ODAE method with other existing methods with a noise level of δ=60. From the table, it is clear that the PNSR value is greater for the proposed method than the others, whereas the value of SSIM and FOM is also high for the ODAE method.

Table 1: The performance comparison of the proposed ODAE method with K-SVD, BM3D, NLM with the noise level of δ = 60 on lena image

Methods used	*δ = 60*		
	PNSR (in dB)	*FOM*	*SSIM*
K-SVD	25.90	0.2398	0.8354
BM3D	26.89	0.3487	0.8676
NLM	26.94	0.3677	0.7777
Proposed ODAE	27.50	0.4598	0.8876

(a) Lena (b) Airplane (c) Monarch (d) Baboon

Figure 1: The standard benchmark images (a) Monarch, (b) Airplane, (c) Lena, (d) Baboon

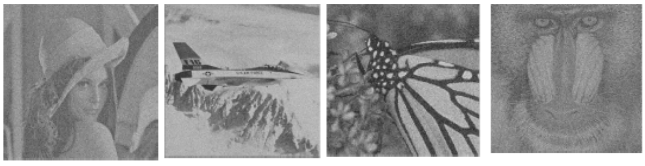

(a) Lena (b) Airplane (c) Monarch (d) Baboon

Figure 2: The four noise-destroyed images of (a) Lena, (b) Airplane, (c) Monarch, (d) Baboon

Table 2: The performance comparison of the proposed ODAE method with K-SVD, BM3D, NLM with the noise level of δ=60 on airplane image

Methods used	*δ=60*		
	PNSR (in dB)	*FOM*	*SSIM*
K-SVD	29.79	0.7231	0.8659
BM3D	30.44	0.7319	0.7754
NLM	28.66	0.5996	0.8832
Proposed ODAE	31.34	0.7742	0.8976

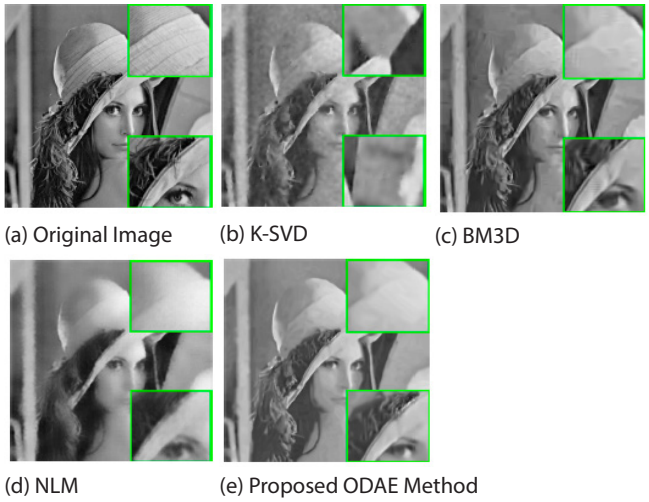

(a) Original Image (b) K-SVD (c) BM3D

(d) NLM (e) Proposed ODAE Method

Figure 3: The comparison of the denoising results of Lena noisy image with noise level of $\delta = 60$. The results images are (a) Original Image, (b) K-SVD, (c) BM3D, (d) NLM and (e) Proposed ODAE method.

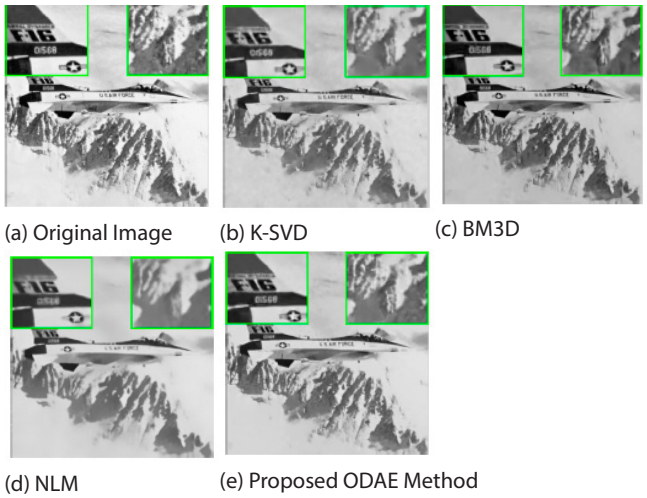

(a) Original Image (b) K-SVD (c) BM3D

(d) NLM (e) Proposed ODAE Method

Figure 4: The comparison of the denoising results of Airplane noisy image with noise level of δ = 60. The results images are (a) Original Image, (b) K-SVD, (c) BM3D, (d) NLM and (e) Proposed ODAE method

(a) Original Image (b) K-SVD (c) BM3D

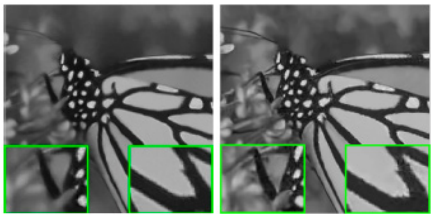

(d) NLM (e) Proposed ODAE Method

Figure 5: The comparison of the denoising results of Monarch noisy image with noise level of δ = 60. The results images are (a) Original Image, (b) K-SVD, (c) BM3D, (d) NLM and (e) Proposed ODAE method

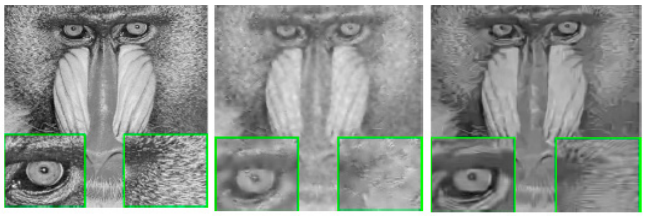

(a) Original Image (b) K-SVD (c) BM3D

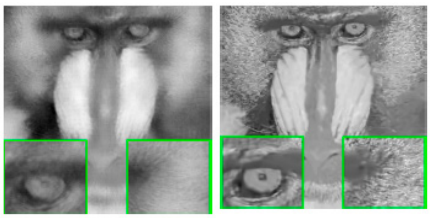

(d) NLM (e) Proposed ODAE Method

Figure 6: The comparison of the denoising results of Baboon's noisy image with noise level of δ = 60. The results images are (a) Original Image, (b) K-SVD, (c) BM3D, (d) NLM and (e) Proposed ODAE method

Table 3: The performance comparison of the Proposed ODAE Method with K-SVD, BM3D, NLM with the noise level of δ = 60 on Monarch Image

Methods used	*δ = 60*		
	PNSR (in dB)	*FOM*	*SSIM*
K-SVD	27.27	0.8352`	0.8780
BM3D	28.83	0.8072	0.8001
NLM	25.34	0.7080	0.7789
Proposed ODAE	29.54	0.9001	0.9042

Table 4: The performance comparison of the proposed ODAE Method with K-SVD, BM3D, NLM with the noise level of δ=60 on Baboon image

Methods used	*δ = 60*		
	PNSR (in dB)	*FOM*	*SSIM*
K-SVD	21.89	0.3465	0.4563
BM3D	20.89	0.3037	0.4876
NLM	19.98	0.2589	0.3578
Proposed ODAE	23.65	0.3485	0.5001

Table 3 depicts the performance comparison of the proposed ODAE method with other existing methods with a noise level of δ=60. From the table, it is clear that the PNSR value (29.54) is greater for the proposed method than the others, whereas the value of SSIM (0.9042) and FOM (0.9001) is also high for the ODAE method.

The following Table 4 depicts the performance comparison of the proposed ODAE method with other existing methods with a noise level of δ=60. From the table, it is clear that the PNSR value (23.65) is greater for the proposed method than the others, whereas the values of SSIM (0.5001) and FOM (0.3485) is also high for the ODAE method.

From the tables, it is clear that the proposed ODAE method gives the maximum value of PNSR, FOM and SSIM on all four images with a noise level of δ=60.

Tables 5a, b and c represent the values of PNSR, SSIM and FOM with the different noise levels for the given methods by using Lena image (Figure 3). From Table 5a, at the noise level of 15 and 25, the method BM3D gives the maximum value of PNSR, and the proposed method gives the maximum value only on the noise level of 5, 40, and 60. In Table 5b, the method BM3D gives the maximum value of SSIM at the noise level of 5, whereas the proposed method generates the maximum value at 15, 25, 40 and 60. In Table 5c, at the noise of 15, BM3D method gives the maximum value of FOM, and the proposed method produces the maximum value at the noise levels of 5, 25, 40 and 60. It is concluded that the performance metrics gives the maximum values only at the noise level of 60 by the proposed ODAE Method for the given Lena image.

Tables 6a, b and c represent the values of PNSR, SSIM and FOM with the different noise levels for the given methods by using an airplane image (Figure 4). From Table 6a, at all the noise levels, the proposed ODAE method gives the maximum value of PNSR. In Table 6b, the value of SSIM reaches the maximum in the proposed method at all the noise level. In Table 6c, at the noise of 15 and 25, BM3D method gives the maximum value of FOM, and proposed method produces the maximum value at the noise levels of 5, 40 and 60. It is concluded that the performance metrics give the maximum values only at the noise level of 60 by the proposed ODAE Method for a given Airplane image.

Tables 7a, b and c represent the values of PNSR, SSIM and FOM with the different noise levels for the given methods by using Monarch image (Figure 5). From Table 7a, at the noise

Table 5a: Performance analysis of PNSR value for K-SVD, BM3D, NLM and proposed ODAE method with different noise levels on lena image

Level of Noise (δ)	Methods used			
	K-SVD	BM3D	NLM	Proposed ODAE
5	38.62	38.71	37.17	38.74
15	33.73	34.25	31.45	34.12
25	31.34	32.05	28.73	31.98
40	29.06	29.86	26.53	29.92
60	25.90	26.89	26.94	27.50

Table 5b: Performance analysis of SSIM (Structural Similarity) value for K-SVD, BM3D, NLM and Proposed ODAE method with different noise levels on lena image

Level of Noise (δ)	Methods used			
	K-SVD	BM3D	NLM	Proposed ODAE
5	0.9125	0.9303	0.9113	0.9289
15	0.7552	0.7920	0.6457	0.8093
25	0.6420	0.6885	0.4242	0.7178
40	0.4858	0.5677	0.3266	0.5769
60	0.2398	0.3487	0.3677	0.4598

Table 5c: Performance analysis of FOM (Figure of Merit) value for K-SVD, BM3D, NLM and proposed ODAE method with different noise levels on lena image

Level of Noise (δ)	Methods used			
	K-SVD	BM3D	NLM	Proposed ODAE
5	0.9455	0.9444	0.9239	0.9450
15	0.8860	0.8953	0.8454	0.8928
25	0.8428	0.8607	0.7964	0.8615
40	0.7928	0.8159	0.7511	0.8253
60	0.8354	0.8676	0.7777	0.8876

Table 6a: Performance analysis of PNSR value for K-SVD, BM3D, NLM and Proposed ODAE method with different noise levels on airplane image

Level of Noise (δ)	Methods used			
	K-SVD	BM3D	NLM	Proposed ODAE
5	39.07	39.25	37.40	39.31
15	33.60	33.89	31.31	33.97
25	30.97	31.44	28.17	31.45
40	28.53	29.06	25.32	29.13
60	29.79	30.44	28.66	31.34

Table 6b: Performance analysis of SSIM value for K-SVD, BM3D, NLM and proposed ODAE method with different noise levels on airplane image

Level of Noise (δ)	Methods used			
	K-SVD	BM3D	NLM	Proposed ODAE
5	0.9251	0.9331	0.9278	0.9388
15	0.8095	0.8240	0.7677	0.8482
25	0.7306	0.7419	0.6036	0.7638
40	0.6135	0.6570	0.4750	0.6792
60	0.7231	0.7231	0.5996	0.7742

Table 6c: Performance analysis of figure of merit (FOM) value for K-SVD, BM3D, NLM and proposed ODAE method with different noise levels on airplane image

Level of Noise (δ)	Methods used			
	K-SVD	BM3D	NLM	Proposed ODAE
5	0.9584	0.9595	0.9425	0.9598
15	0.9100	0.9162	0.8756	0.9160
25	0.8719	0.8833	0.8286	0.8801
40	0.8231	0.8401	0.7797	0.8515
60	0.8659	0.7754	0.8832	0.8976

Table 7a: Performance analysis of PNSR value for K-SVD, BM3D, NLM and proposed ODAE method with different noise levels on monarch image

Level of Noise (δ)	Methods used			
	K-SVD	BM3D	NLM	Proposed ODAE
5	37.74	38.25	36.72	38.29
15	31.45	31.97	29.73	32.10
25	28.72	29.31	26.43	29.44
40	26.56	26.72	27.03	26.77
60	27.27	28.83	25.34	29.54

Table 7b: Performance analysis of SSIM value for K-SVD, BM3D, NLM and proposed ODAE method with different noise levels on monarch image

Level of Noise (δ)	Methods used			
	K-SVD	BM3D	NLM	Proposed ODAE
5	0.9738	0.9762	0.9789	0.9751
15	0.9226	0.9281	0.9397	0.9386
25	0.8532	0.8821	0.8066	0.9076
40	0.8143	0.8259	0.8537	0.8128
60	0.8780	0.8780	0.7789	0.9042

level of 5, 15, 25 and 60 give the maximum value of PNSR by the proposed method, whereas the noise level 40, the NLM method gives the maximum value. In Table 7b, the proposed method gives the higher value of SSIM at the noise level of 25 and 60, whereas at the noise level of 15 and 40, NLM method gives the maximum value and at the noise level 5, BM3D method gives a higher value. In Table 7c, at the noise of 5, 15 and 40, the BM3D method gives the maximum value of FOM, and the proposed method produces the maximum value at the noise levels of 25 and 60. It is concluded that

Table 7c: Performance analysis of FOM value for K-SVD, BM3D, NLM and proposed ODAE method with different noise levels on monarch image

Level of Noise (δ)	*Methods used*			
	K-SVD	*BM3D*	*NLM*	*Proposed ODAE*
5	0.9720	0.9756	0.9677	0.9748
15	0.9282	0.9384	0.8999	0.9307
25	0.8880	0.9031	0.8336	0.9045
40	0.8344	0.8585	0.7517	0.8421
60	0.8780	0.8001	0.7789	0.9042

Table 8a: Performance analysis of PNSR value for K-SVD, BM3D, NLM and proposed ODAE method with different noise levels on baboon image

Level of noise (δ)	*Methods used*			
	K-SVD	*BM3D*	*NLM*	*Proposed ODAE*
5	35.44	35.49	34.48	34.59
15	28.42	28.67	25.95	28.77
25	25.79	26.04	22.85	26.01
40	23.57	23.88	24.03	24.01
60	21.89	20.89	19.98	23.65

Table 8b: Performance analysis of SSIM value for K-SVD, BM3D, NLM and proposed ODAE method with different noise levels on baboon image

Level of Noise (δ)	*Methods used*			
	K-SVD	*BM3D*	*NLM*	*Proposed ODAE*
5	0.9326	0.9297	0.9123	0.9351
15	0.8234	0.8187	0.7051	0.7995
25	0.7245	0.7174	0.4036	0.7403
40	0.5428	0.5252	0.5865	0.5758
60	0.3465	0.3037	0.2589	0.3485

Table 8c: Performance analysis of FOM value for K-SVD, BM3D, NLM and proposed ODAE method with different noise levels on baboon image

Level of Noise (δ)	*Methods used*			
	K-SVD	*BM3D*	*NLM*	*Proposed ODAE*
5	0.9536	0.9534	0.9288	0.9519
15	0.8227	0.8327	0.8421	0.8388
25	0.7081	0.7300	0.7483	0.7500
40	0.5570	0.6029	0.6189	0.6057
60	0.4563	0.4876	0.3578	0.5001

the performance metrics gives the maximum values only at the noise level of 60 by the proposed ODAE Method for the given Monarch image.

Tables 8a, b and c represent the values of PNSR, SSIM and FOM with the different noise levels for the given methods by using Monarch image (Figure 6). From Table 8a, at the noise level of 5, 25 BM3D gives the maximum value of PNSR, whereas the noise level 40, NLM method gives the maximum value and the proposed method gives a higher value at the noise level of 15 and 60. In Table 8b, the proposed method gives a higher value of SSIM at the noise levels of 5, 25 and 60, whereas at the noise level of 15 K-SVD gives a higher value and 40, NLM method gives the maximum. In Table 8c, at the noise of 5 BM3D method give the maximum value of FOM, and the proposed method produces the maximum value at the noise levels of 25 and 60 and at the noise level of 15 and 40 NLM gives the higher value. It is concluded that the performance metrics gives the maximum values only at the noise level of 60 by the proposed ODAE Method for given Monarch image.

Conclusion

The proposed integration of denoising autoencoders (DAEs) with CSO provides a powerful and effective framework for image denoising and quality enhancement. By combining the strengths of DAEs in feature extraction and noise removal with the optimization capabilities of CSO, this approach effectively minimizes reconstruction error, yielding cleaner, high-quality images from noisy data.

The use of CSO to optimize the DAE's weights and biases addresses common issues of overfitting and local minima, enhancing the denoising model's robustness and generalization. CSO's ability to dynamically balance exploration and exploitation through Levy flights allows the DAE to achieve a more global search for optimal parameters, leading to improved denoising results across various noise types and levels.

Experimental results indicate that the optimized DAE-CSO model achieves higher reconstruction quality, as validated by metrics like PSNR and SSIM. This improvement in visual quality makes the model highly suitable for applications in computer vision, medical imaging, and remote sensing, where image clarity and detail preservation are critical.

Overall, the proposed DAE-CSO method represents a robust, adaptable solution for image quality assessment and denoising, demonstrating its potential as a valuable tool in image processing and related fields. Future work can further enhance this framework by exploring hybrid optimization strategies, expanding noise types, and optimizing computational efficiency to meet real-time processing needs.

References

Al-Abaji, M. A. (2021). Cuckoo search algorithm: review and its application. *Tikrit Journal of Pure Science*, 26(2), 137-144.

Cui, H., & Zdeborová, L. (2023). High-dimensional asymptotics of denoising autoencoders. *Advances in Neural Information Processing Systems*, 36, 11850-11890.

Do, Y., Cho, Y., Kang, S. H., & Lee, Y. (2022). Optimization of block-

matching and 3D filtering (BM3D) algorithm in brain SPECT imaging using fan beam collimator: Phantom study. *Nuclear Engineering and Technology*, 54(9), 3403-3414.

Gheller, C., & Vazza, F. (2022). Convolutional deep denoising autoencoders for radio astronomical images. *Monthly Notices of the Royal Astronomical Society*, 509(1), 990-1009.

Guo, H., Bin, Y., Hou, Y., Zhang, Q., & Luo, H. (2021). Iqma network: Image quality multi-scale assessment network. *In Proceedings of the IEEE/CVF Conference on Computer Vision and Pattern Recognition* (pp. 443-452).

Hossain, M. M., Hasan, M. M., Rahim, M. A., Rahman, M. M., Yousuf, M. A., Al-Ashhab, S., ... & Moni, M. A. (2022). Particle swarm optimized fuzzy CNN with quantitative feature fusion for ultrasound image quality identification. *IEEE Journal of Translational Engineering in Health and Medicine*, 10, 1-12.

Kumar, V. S., & Jayalakshmi, V. (2021, September). Reconstructing the Medical Image by Autoencoder with Stochastic Processing in Neural Network. I*n 2021 Third International Conference on Inventive Research in Computing Applications (ICIRCA)* (pp. 1521-1526). IEEE.

Lee, W. H., Ozger, M., Challita, U., & Sung, K. W. (2021). Noise learning-based denoising autoencoder. *IEEE Communications Letters*, 25(9), 2983-2987.

Ma, K., & Fang, Y. (2021, October). Image quality assessment in the modern age. *In Proceedings of the 29th ACM International Conference on Multimedia* (pp. 5664-5666).

Merzougui, N., & Djerou, L. (2021). Multi-gene Genetic Programming based Predictive Models for Full-reference Image Quality Assessment. *Journal of Imaging Science & Technology*, 65(6).

Mohiz, M. J., Baloch, N. K., Hussain, F., Saleem, S., Zikria, Y. B., & Yu, H. (2021). Application mapping using cuckoo search optimization with Lévy flight for NoC-based system. IEEE Access, 9, 141778-141789.

Sharma, A., Sharma, A., Chowdary, V., Srivastava, A., & Joshi, P. (2021). Cuckoo search algorithm: A review of recent variants and engineering applications. *Metaheuristic and Evolutionary Computation: Algorithms and Applications*, 177-194.

Tian, Y., Zhang, Y., & Zhang, H. (2023). Recent advances in stochastic gradient descent in deep learning. *Mathematics*, 11(3), 682.

WangNo, N., Chiewchanwattana, S., & Sunat, K. (2023). An efficient adaptive thresholding function optimized by a cuckoo search algorithm for a despeckling filter of medical ultrasound images. *Journal of Ambient Intelligence and Humanized Computing*, 1-26.

Žalik, K. R., & Žalik, M. (2023, July). Comparison of K-means, K-means++, X-means and Single Value Decomposition for Image Compression. *In 2023 27th International Conference on Circuits, Systems, Communications and Computers (CSCC)* (pp. 295-301). IEEE.

Zhang, X. (2022). Two-step non-local means method for image denoising. *Multidimensional Systems and Signal Processing*, 33(2), 341-366.